# Splitting techniques with staggered grids for the Navier-Stokes equations

Heike Haschke, Wilhelm Heinrichs

*Universität GH Essen, Ingenieurmathematik (FB 10) Universitätsstr. 3, D-45117 Essen, Germany*

**Abstract** A pseudo spectral approximation for the Navier-Stokes equations is presented using a new splitting technique based on the Uzawa algorithm. The system is decoupled into Helmholtz equations for the velocity and an equation with the Pseudo-Laplacian for the pressure. Staggered grids with Gauss- and Gauss-Lobatto nodes are employed. Preconditioning with finite differences is considered. By extrapolation a stable second order method in time can be achieved.

## 1 Introduction

We present a pseudo spectral approximation for the Navier-Stokes equations. First the unsteady Stokes equations are considered. Using the Uzawa algorithm the spectral system is decoupled into Helmholtz equations for the velocity components and into an equation with the Pseudo-Laplacian for the pressure. In order to avoid spurious modes the pressure is approximated by polynomials of one degree less than those used for the velocity. Two grids are used by taking the Gauss nodes for the pressure and the standard Chebyshev Gauss-Lobatto nodes for the velocity. The Gauss nodes were mainly chosen for accomplishing an analysis of the spectral method. We also prove that the eigenvalues of the spectral Pseudo-Laplacian are real and negative (except of one eigenvalue which is zero and belongs to the constant mode). Since the spectral Pseudo-Laplacian is very ill-conditioned we present suitable finite difference (FD) preconditioners for an effective iterative solver.
In the time discretization a high order backward differentiation scheme for the intermediate velocity is combined with a high order extrapolant for the pressure. It is numerically shown that a stable second order method in time can be achieved.

## 2 Time splitting scheme

We consider the unsteady Stokes equations

$$\begin{aligned} \frac{\partial u}{\partial t} - \nabla^2 u + \nabla p &= f \text{ in } \Omega = (-1,1)^2, && (2.1)\\ \nabla \cdot u &= 0 \text{ in } \Omega, && (2.2)\\ u &= 0 \text{ on } \partial\Omega, && (2.3) \end{aligned}$$

where $u = (u_1, u_2)^t$ denotes the velocity and $p$ the pressure. $f : \Omega \to \mathbb{R}^2$ is a given force. We impose the average pressure to be zero, i.e.

$$\int_\Omega p dx = 0,$$

as the pressure is only determined up to a constant.
The standard backward Euler time discretization of equations (2.1)-(2.3) leads to the following scheme:

$$
\begin{aligned}
L^n_{t,k} u^{n+1} - \nabla^2 u^{n+1} + \nabla p^{n+1} &= f^{n+1} \text{ in } \Omega, &(2.4)\\
\nabla \cdot u^{n+1} &= 0 \text{ in } \Omega, &(2.5)\\
u^{n+1} &= 0 \text{ on } \partial\Omega, &(2.6)
\end{aligned}
$$

where $\triangle t$ denotes the step size in $t$ and the index $n+1$ indicates that the functions are evaluated at the time step $t_n = n \cdot \triangle t$. $L^n_{t,k}$ represents the backward differentation scheme for the approximation of $\frac{\partial}{\partial t}$ and $k$ is the order of the scheme. $L^n_{t,k}$ can be written as:

$$
L^n_{t,k} u^{n+1} = \frac{1}{\triangle t} \sum_{m=0}^{k} \beta_m u^{n+1-m}.
$$

For $k = 1$ the standard backward Euler scheme is given by $\beta_0 = 1$, $\beta_1 = -1$ and we obtain:

$$
L^n_{t,1} u^{n+1} = \frac{u^{n+1} - u^n}{\triangle t}.
$$

This algorithm is of first order in time.
A second order scheme can be obtained for $k = 2$ using $\beta_0 = \frac{3}{2}$, $\beta_1 = -2$, $\beta_2 = \frac{1}{2}$:

$$
L^n_{t,2} u^{n+1} = \frac{\frac{3}{2}u^{n+1} - 2u^n + \frac{1}{2}u^{n-1}}{\triangle t}.
$$

Finally a method of third order for $k = 3$ is given applying $\beta_0 = \frac{11}{6}$, $\beta_1 = -3$, $\beta_2 = \frac{3}{2}$ and $\beta_3 = -\frac{1}{3}$.
To minimize the computational cost we introduce the following splitting scheme in which we have separate equations for the velocity and the pressure. We obtain:

$$
\begin{aligned}
L^n_{t,k} \tilde{u}^{n+1} - \nabla^2 \tilde{u}^{n+1} + \nabla \bar{p}^{n+1}_l &= f^{n+1} \text{ in } \Omega, &(2.7)\\
\tilde{u}^{n+1} &= 0 \text{ on } \partial\Omega, &(2.8)
\end{aligned}
$$

and

$$
\begin{aligned}
\beta_0 \frac{u^{n+1} - \tilde{u}^{n+1}}{\triangle t} + \nabla(p^{n+1} - \bar{p}^{n+1}_l) &= 0 \text{ in } \Omega, &(2.9)\\
\nabla \cdot u^{n+1} &= 0 \text{ in } \Omega, &(2.10)\\
u^{n+1} \cdot \nu &= 0 \text{ on } \partial\Omega. &(2.11)
\end{aligned}
$$

Here $\nu$ denotes the outer unit normal, $\tilde{u}^{n+1}$ an intermediate velocity and $\bar{p}^{n+1}_l$ an extrapolant for the pressure obtained from the previous $l$ time steps.
Obviously the order of convergence depends on the order $k$ of the backward differentiation scheme and on the order $l$ of the extrapolation where

$$
\bar{p}^{n+1}_l = \sum_{m=0}^{l-1} \gamma_m p^{n-m},
$$

the values $\gamma_m$, $m = 0, \ldots, l-1$, being suitable coefficients. For $l = 1$ we use especially $\gamma_0 = 1$, for $l = 2$ we have $\gamma_0 = 2$, $\gamma_1 = -1$.

Let

$$\tilde{f}^{n+1} = f^{n+1} - \frac{1}{\triangle t} \sum_{m=1}^{k} \beta_m u^{n+1-m} - \nabla \bar{p}_l^{n+1}.$$

(2.7)-(2.8) is essentially equivalent to the following Helmholtz problem:

$$\left(-\nabla^2 + \beta_0 \frac{1}{\triangle t} I\right) \tilde{u}^{n+1} = \tilde{f}^{n+1} \text{ in } \Omega, \tag{2.12}$$

$$\tilde{u}^{n+1} = 0 \text{ on } \partial\Omega. \tag{2.13}$$

The system (2.9)-(2.11) corresponds to:

$$\beta_0 \frac{1}{\triangle t} u^{n+1} + \nabla p^{n+1} = g^{n+1} \text{ in } \Omega, \tag{2.14}$$

$$\nabla \cdot u^{n+1} = 0 \text{ in } \Omega, \tag{2.15}$$

$$u^{n+1} \cdot \nu = 0 \text{ on } \partial\Omega, \tag{2.16}$$

where $g^{n+1} = \beta_0 \frac{1}{\triangle t} \tilde{u}^{n+1} + \nabla \bar{p}_l^{n+1}$. From now on we will consider (2.14)-(2.16).

# 3 Pseudo spectral discretization

In order to give a pseudo spectral discretization of the Stokes systems we have to define spectral operators for the velocity and the pressure. This is done in the one-dimensional case first. In the two-dimensional case we get the corresponding operators by tensor product representation. For $N \in \mathbb{N}$ let $\mathbb{P}_N$ be the space of polynomials of degree $\leq N$, while $\mathbb{P}_N^0$ is the space of polynomials in $\mathbb{P}_N$ which in addition fulfill the homogeneous Dirichlet boundary conditions. We approximate $u$ by polynomials in $\mathbb{P}_N^0$ and $p$ by polynomials in $\mathbb{P}_{N-1}$. We apply staggered grids where the velocity is defined at the Gauss-Lobatto nodes $(x_i, y_j) = \left(\cos \frac{i\pi}{N}, \cos \frac{j\pi}{N}\right)$, $i, j = 0, \ldots, N$, while the pressure is evaluated at the Gauss nodes $(z_i, w_j) = \left(\cos \frac{(2i-1)\pi}{2N}, \cos \frac{(2j-1)\pi}{2N}\right)$, $i, j = 1, \ldots, N$. We only consider even $N$. For odd $N$ a similar treatment is possible.
Here we use the pseudo spectral Chebyshev discretization. The corresponding spectral derivative operator for the velocity components can be found in [1].
After eliminating the boundary conditions we obtain

$$u'(x_j) \cong (\hat{D}_u^0 u)_j, \quad j = 0, \ldots, N,$$

where $\hat{D}_u^0 \in \mathbb{R}^{N+1, N-1}$, $x_j = \cos \frac{j\pi}{N}$, $j = 0, \ldots, N$.
Now we have to interpolate between the Gauss-Lobatto and the Gauss nodes. If $T \in \mathbb{R}^{N, N+1}$ denotes the interpolation matrix we derive:

$$u'(z_j) \cong (T \hat{D}_u^0 u)_j, \quad j = 1, \ldots, N.$$

The operator $D^0 = T\hat{D}_u^0 \in \mathbb{R}^{N, N-1}$ represents the first derivative operator.
The second derivative is considered at the Gauss-Lobatto nodes and reads:

$$u''(x_j) \cong ((D_u^2)^0 u)_j, \quad j = 1, \ldots, N-1,$$

where $(D_u^2)^0 \in \mathbb{R}^{N-1, N-1}$.

Now let us define the derivative operator for the pressure. Note that one has to interpolate between the Gauss and the Gauss-Lobatto nodes. We get:

$$p'(x_j) \cong (Dp)_j, \quad j = 1, \ldots, N-1,$$

where $D \in \mathrm{I\!R}^{N-1,N}$ is given by:

$$D = T_{p_1} \hat{D}_p T_{p_2}.$$

$T_{p_2} \in \mathrm{I\!R}^{N,N}$ interpolates into $\mathrm{I\!P}_{N-1}$, $\hat{D}_p \in \mathrm{I\!R}^{N,N}$ performs the differentiation in the coefficient space and $T_{p_1} \in \mathrm{I\!R}^{N-1,N}$ transforms back in the physical space. So we transform directly onto the Gauss-Lobatto nodes.
$\hat{D}_p = (d_{i,j})_{i,j=1,\ldots,N}$ is explicitly defined as:

$$d_{i,j} = \begin{cases} \frac{2(j-1)}{c_i}, & j = i+1, i+3, \ldots, N-1 \\ 0, & \text{else} \end{cases}$$

$$c_i = \begin{cases} 2, & i = 1 \\ 1, & \text{else.} \end{cases}$$

For the two-dimensional space we calculate the derivative operators by the tensor product representation. We can introduce the partial differential operators for the velocity as follows:

$$\frac{\partial}{\partial x} : \; D_x^0 = D^0 \otimes I, \quad \frac{\partial}{\partial y} : \; D_y^0 = I \otimes D^0,$$

$$\frac{\partial^2}{\partial x^2} : \; D_{xx}^0 = (D_u^2)^0 \otimes I, \quad \frac{\partial^2}{\partial y^2} : \; D_{yy}^0 = I \otimes (D_u^2)^0,$$

$$\frac{\partial^2}{\partial x^2} + \frac{\partial^2}{\partial y^2} : \; D_\triangle^0 = (D_{xx}^0 + D_{yy}^0),$$

where $I \in \mathrm{I\!R}^{N,N}$ denotes the identity matrix. This induces: $D_x^0, D_y^0 \in \mathrm{I\!R}^{N^2,(N-1)\cdot N}$.
For the pressure we work analogously:

$$\frac{\partial}{\partial x} : \; D_x = D \otimes I, \quad \frac{\partial}{\partial y} : \; D_y = I \otimes D.$$

where $D_x, D_y \in \mathrm{I\!R}^{(N-1)\cdot N, N^2}$.
Note that the transform is only done in one variable from Gauss-Lobatto to Gauss nodes respectively vice versa. Therefore we need a new definition for the pseudo spectral discretization. For the velocity it means:

$$\frac{\partial}{\partial x_G} : \; D_{x,G}^0 = D^0 \otimes T, \quad \frac{\partial}{\partial y_G} : \; D_{y,G}^0 = T \otimes D^0,$$

and for the pressure we use

$$\frac{\partial}{\partial x_{GL}} : \; D_{x,GL} = D \otimes (T_{p_1} \cdot T_{p_2}), \quad \frac{\partial}{\partial y_{GL}} : \; D_{y,GL} = (T_{p_1} \cdot T_{p_2}) \otimes D.$$

The index $G$ indicates that we transform onto the Gauss nodes (analogously: $GL$).
Now we are able to provide the pseudo spectral discretization for the Stokes problem. First we consider (2.4)-(2.6):

$$\begin{aligned}
\left(-D^0_\triangle + \beta_0 \frac{1}{\triangle t} I\right) u_1^{n+1} + D_{x,GL} p^{n+1} &= \hat{f}_1^{n+1} \ \text{ in } \Omega, && (3.1)\\
\left(-D^0_\triangle + \beta_0 \frac{1}{\triangle t} I\right) u_2^{n+1} + D_{y,GL} p^{n+1} &= \hat{f}_2^{n+1} \ \text{ in } \Omega, && (3.2)\\
D^0_{x,G} u_1^{n+1} + D^0_{y,G} u_2^{n+1} &= 0 \ \text{ in } \Omega, && (3.3)\\
u_1^{n+1} = u_2^{n+1} &= 0 \ \text{ on } \partial\Omega, && (3.4)
\end{aligned}$$

where

$$\hat{f}_i^{n+1} = f_i^{n+1} - \frac{1}{\triangle t} \sum_{m=1}^{k} \beta_m u_i^{n+1-m} \quad (i = 1, 2).$$

Since we would like to use the operator splitting we have to solve a Helmholtz problem for the intermediate velocity components which reads

$$\begin{aligned}
\left(-D^0_\triangle + \beta_0 \frac{1}{\triangle t} I\right) \tilde{u}_i^{n+1} &= \tilde{f}_i^{n+1} \ \text{ in } \Omega, && (3.5)\\
\tilde{u}_i^{n+1} &= 0 \text{ on } \partial\Omega, \quad i = 1, 2, && (3.6)
\end{aligned}$$

and

$$\begin{aligned}
\beta_0 \frac{1}{\triangle t} u_1^{n+1} + D_{x,GL} p^{n+1} &= g_1^{n+1} \ \text{ in } \Omega, && (3.7)\\
\beta_0 \frac{1}{\triangle t} u_2^{n+1} + D_{y,GL} p^{n+1} &= g_2^{n+1} \ \text{ in } \Omega, && (3.8)\\
D^0_{x,G} u_1^{n+1} + D^0_{y,G} u_2^{n+1} &= 0 \text{ in } \Omega, && (3.9)\\
u_1^{n+1} = u_2^{n+1} &= 0 \text{ on } \partial\Omega. && (3.10)
\end{aligned}$$

By applying the divergence to the first two equations and further using the divergence-free condition (Uzawa decoupling) we finally obtain:

$$\left(D^0_{x,G} D_{x,GL} + D^0_{y,G} D_{y,GL}\right) p^{n+1} = D^0_{x,G} g_1^{n+1} + D^0_{y,G} g_2^{n+1}. \tag{3.11}$$

The operator $B \in \mathbb{R}^{N^2,N^2}$ with

$$\begin{aligned}
B &= D^0_{x,G} D_{x,GL} + D^0_{y,G} D_{y,Gl}\\
&= D^0_x D_x + D^0_y D_y.
\end{aligned}$$

is called the *Pseudo-Laplacian* or *energy*.

# 4 Properties of the spectral Pseudo-Laplacian

In this section we consider the Pseudo-Laplacian

$$B = D^0_x D_x + D^0_y D_y = A \otimes I + I \otimes A.$$

First we consider the one-dimensional Pseudo-Laplacian

$$A = D^0 D.$$

We are interested in its eigenvalues which are calculated numerically. Therefore we define

$$\begin{aligned}
\lambda_{min} &= \min\{|\lambda| \mid \lambda \neq 0 \text{ eigenvalue of } A\} \\
\lambda_{max} &= \max\{|\lambda| \mid \lambda \neq 0 \text{ eigenvalue of } A\}.
\end{aligned}$$

In table 4.1 we present the maximal and the minimal eigenvalues $\lambda_{min}$ and $\lambda_{max}$ of $A$.
It is numerically shown that $\lambda_{min}$ and $\lambda_{max}$ of $A$ have a similar behaviour as the eigenvalues of $(D^2)^0$. For increasing $N$ the minimal eigenvalue $\lambda_{min}$ approximates $\pi^2/4$.

**Table 4.1**

$\lambda_{min}$ and $\lambda_{max}$ of $A$

| $N$ | $\lambda_{min}$ | $\lambda_{max}$ | $\lambda_{max}/N^3$ |
|---|---|---|---|
| 4 | 2.4560 | $1.9544 \cdot 10^1$ | 0.3054 |
| 8 | 2.4674 | $2.1437 \cdot 10^2$ | 0.4187 |
| 16 | 2.4674 | $3.1748 \cdot 10^3$ | 0.7751 |
| 32 | 2.4674 | $4.9939 \cdot 10^4$ | 1.5240 |
| 64 | 2.4674 | $7.9573 \cdot 10^5$ | 3.0355 |
| 128 | 2.4674 | $1.2719 \cdot 10^7$ | 6.0649 |

Table 4.2 presents $\lambda_{min}$ and $\lambda_{max}$ for the two-dimensional operator $B$.

**Table 4.2**

$\lambda_{min}$ and $\lambda_{max}$ of $B$

| $N$ | $\lambda_{min}$ | $\lambda_{max}$ | $\lambda_{max}/N^3$ |
|---|---|---|---|
| 4 | 2.4560 | $3.9088 \cdot 10^1$ | 0.6108 |
| 8 | 2.4674 | $4.2874 \cdot 10^2$ | 0.8374 |
| 16 | 2.4674 | $6.3496 \cdot 10^3$ | 1.5502 |

For an analysis of $A$ we introduce a somewhat different representation of $A$. Let $p$ be a polynomial in $\mathbb{P}_{N-1}$. Applying $A$ to $p$ is equivalent to first applying $D$ to $P$ and then $D^0$ to $Dp$. We obtain:

$$p'(x_j) = (Dp)_j, \quad j = 1, \dots, N-1,$$

where we deal with $p$ as a vector in $\mathbb{R}^N$.
Before applying $D^0$ to $Dp$ we have to map $p'$ onto a polynomial $p_0' \in \mathbb{P}_N^0$ which is defined by

$$p_0'(x_j) = p'(x_j), \quad j = 1, \dots, N-1.$$

Obviously, $p_0'$ can explicitly be written as

$$p_0' = p' + \alpha T_N' + \beta x T_N', \tag{4.1}$$

where $T_N$ denotes the $N$th Chebyshev polynomial.
$\alpha$ and $\beta$ are determined such that $p_0'(1) = p_0'(-1) = 0$, i.e.,

$$\begin{aligned} \alpha &= \frac{1}{2N^2}\left(p'(-1) - p'(1)\right), \\ \beta &= -\frac{1}{2N^2}\left(p'(-1) + p'(1)\right). \end{aligned}$$

Applying $D^0$ to $Dp$ is equivalent to taking the first derivative of $p_0'$, i.e.:

$$p_0'' = p'' + \alpha T_N'' + \beta (xT_N')'. \tag{4.2}$$

We derive

$$\begin{aligned} (Ap)_j &= p''(z_j) + \alpha T_N''(z_j) + \beta (xT_N')'(z_j) \\ &= p''(z_j) + \frac{1}{2N^2}\left(p'(-1) - p'(1)\right) T_N''(z_j) - \frac{1}{2N^2}\left(p'(-1) + p'(1)\right) \cdot (xT_N')'(z_j) \\ &= p''(z_j) + \frac{1}{2N^2} p'(-1) \cdot \left(T_N''(z_j) \cdot (1 - z_j) - T_N'(z_j)\right) \\ &\quad - \frac{1}{2N^2} p'(1)\left(T_N''(z_j) \cdot (1 + z_j) + T_N'(z_j)\right), \end{aligned}$$

where $z_j$ are the Gauss nodes for $j = 1, \ldots, N$.
Knowing that

$$\begin{aligned} T_N'(z_j) &= (-1)^j \cdot N \cdot \frac{1}{\sqrt{1 - z_j^2}} \quad \text{and} \\ T_N''(z_j) &= (-1)^j \cdot N \cdot \frac{z_j}{(1 - z_j^2)^{3/2}}, \end{aligned}$$

it follows for $(Ap)_j$ with $j = 1, \ldots, N$:

$$(Ap)_j = p''(z_j) + \frac{1}{2N} p'(-1) \frac{(-1)^{j+1}(1 - z_j)}{(1 - z_j^2)^{3/2}} + \frac{1}{2N} p'(1) \frac{(-1)^{j+1}(1 + z_j)}{(1 - z_j^2)^{3/2}}. \tag{4.3}$$

In order to represent $A$ in matrix notation, we introduce two diagonal matrices $D_-, D_+ \in R^{N,N}$,

$$\begin{aligned} D_- &= diag(d_{j,j}^-)_{j=1,\ldots,N} : \ d_{j,j}^- = \frac{(-1)^{j+1}(1 - z_j)}{(1 - z_j^2)^{3/2}}, \qquad j = 1, \ldots, N \\ D_+ &= diag(d_{j,j}^+)_{j=1,\ldots,N} : \ d_{j,j}^+ = \frac{(-1)^{j+1}(1 + z_j)}{(1 - z_j^2)^{3/2}}, \qquad j = 1, \ldots, N. \end{aligned}$$

Furthermore we define two matrices $P_+, P_- \in R^{N,N}$ which represent $p'(1)$, $p'(-1)$. To be more precise

$$\begin{aligned} P_+ &= e_+ f_+^t, \qquad f_+ = e_+^t \hat{D}_p T_{p_2}, \\ P_- &= e_+ f_-^t, \qquad f_- = e_-^t \hat{D}_p T_{p_2}, \end{aligned}$$

where $e_+ = (1, 1, \ldots, 1)^t$, $e_- = (1, -1, \ldots, 1, -1)^t \in \mathbb{R}^N$. Obviously $P_+$ and $P_-$ have rank 1.
Now we are able to give a representation of $A$:

$$A = D^2 + D_- P_- + D_+ P_+. \tag{4.4}$$

We then want to prove that the eigenvalues of $A$ are real.
Let $p \in \mathbb{P}_{N-1}$ be an eigenfunction of $A$ with respect to the eigenvalue $\lambda$. We have

$$p'' + \alpha T_N'' + \beta (x T_N')' - \lambda p \equiv 0. \tag{4.5}$$

First we consider the case $\lambda = 0$. It is easy to see that $p = const. \neq 0$ is an eigenfuction. Furthermore it can be seen that this eigenfunction is the only one. Notice that $p'' \in \mathbb{P}_{N-3}$ but $\alpha T_N'' + \beta (x T_n')' \in \mathbb{P}_{N-1}$. This implies $\alpha = \beta = 0$ inducing

$$p'(-1) = p'(1) = 0.$$

These results immediately imply that $p$ is identical to a constant.
In what follows we consider the case $\lambda \neq 0$, $p \neq const.$ Let us introduce $p_1 \equiv p_1(x, \lambda) \in \mathbb{P}_{N-2}$, $p_2 \equiv p_2(x, \lambda) \in \mathbb{P}_{N-1}$ satisfying

$$\begin{aligned} \lambda p_1 - p_1'' &= T_N'' \\ \lambda p_2 - p_2'' &= (x T_N')'. \end{aligned}$$

We define $p_1$ and $p_2$ by

$$\begin{aligned} p_1 &= \sum_{k=0}^{\infty} \lambda^{-k-1} \frac{\partial^{2k}}{\partial x^{2k}} T_N'' \\ p_2 &= \sum_{k=0}^{\infty} \lambda^{-k-1} \frac{\partial^{2k}}{\partial x^{2k}} (x T_N')', \end{aligned}$$

(see [3]) and $p$ is given by

$$p = \alpha p_1 + \beta p_2.$$

Here $\alpha$, $\beta$ have to be chosen such that

$$\begin{aligned} \left(p_1'(1,\lambda) + T_N'(1)\right) \cdot \alpha + \left(p_2'(1,\lambda) + T_N'(1)\right) \cdot \beta &= 0, \\ \left(p_1'(-1,\lambda) + T_N'(-1)\right) \cdot \alpha + \left(p_2'(-1,\lambda) - T_N'(-1)\right) \cdot \beta &= 0. \end{aligned}$$

This system of equations has a non-trivial solution if and only if the determinant vanishes, i.e.

$$\begin{aligned} &\left[\left(p_1'(1,\lambda) + T_N'(1)\right)\left(-p_2'(-1,\lambda) + T_N'(-1)\right)\right] - \\ &\left[\left(p_1'(-1,\lambda) + T_N'(-1)\right)\left(p_2'(1,\lambda) + T_N'(1)\right)\right] = 0. \end{aligned} \tag{4.6}$$

By using

$$p_1'(-1,\lambda) = -p_1'(1,\lambda) \qquad \text{and} \qquad p_2'(-1,\lambda) = p_2'(1,\lambda)$$

and $T_N'(-1) = -T_N'(1) = -N^2$ we finally arrive at the following two characteristic equations:

$$\begin{aligned} p_1'(1,\lambda) + N^2 &= 0 \\ p_2'(1,\lambda) + N^2 &= 0. \end{aligned}$$

These equations determine $(N-1)$ nonzero eigenvalues since $p_1'$ and $p_2'$ are both polynomials of degree $\frac{N}{2}$ in $\lambda^{-1}$.
For instance for $N = 4$ we obtain the two characteristic equations

$$192 \cdot \lambda^{-1} + 16 = 0, \qquad 768 \cdot \lambda^{-2} + 352\lambda^{-1} + 16 = 0,$$

which give the three eigenvalues $\lambda_1 = 12$, $\lambda_{2,3} = -11 \pm \sqrt{73}$ (see also table 4.1).
Let us introduce

$$f_N(x,\mu) = \sum_{k=0}^{\infty} \mu^k \frac{\partial^{k+1}}{\partial x^{k+1}} T_N(x) \tag{4.7}$$

and

$$g_N(x,\mu) = \sum_{k=0}^{\infty} \mu^{k+1} \frac{\partial^k}{\partial x^k} (xT_N')'(x) + xT_N'(x). \tag{4.8}$$

Now we prove that the roots of $f_N$ and $g_N$ have negative real parts.

**Lemma 4.1** *Let $f_N$ and $g_N$ be defined as in (4.7) and (4.8). Then $f_N(1,\mu)$ and $g_N(1,\mu)$ are Hurwitz polynomials.*

*Proof:* The proof for $f_N$ has already been given in [3]. Here we only consider $g_N$. We easily obtain

$$g_N(x,\mu) - \mu \frac{\partial}{\partial x} g_N(x,\mu) = xT_N'(x).$$

Let $w_N(t,\mu) = e^{(1/\mu)t} g_N(x,\mu)$. Then

$$\frac{\partial w_N}{\partial t} - \frac{\partial w_N}{\partial x} = \frac{1}{\mu} \cdot e^{(1/\mu)t} \cdot xT_N'(x),$$

and if $\mu$ is a root of $g_N(1,\mu)$ then $\mu$ is also a root of $w_N$, i.e.

$$w_N(1,t) = 0.$$

Furthermore we know that

$$\frac{1}{\mu} \cdot e^{(1/\mu)t} \cdot x_j T_N'(x_j) = 0, \qquad j = 1, \ldots, N-1,$$

where $x_j$ denote the Chebyshev Gauss-Lobatto nodes. Now it can be shown (see [3]) that $w_N(x,t)$ decreases in time and therefore Re $\mu < 0$. □

Now let

$$f_N^1(\mu) = \sum_{k=0}^{\infty} \mu^{k+1} \frac{\partial^{2k+3}}{\partial x^{2k+3}} T_N(1) + T_N'(1) \tag{4.9}$$

$$f_N^2(\mu) = \sum_{k=0}^{\infty} \mu^{k} \frac{\partial^{2k+2}}{\partial x^{2k+2}} T_N(1) \tag{4.10}$$

and

$$g_N^1(\mu) = \sum_{k=0}^{\infty} \mu^{k+1} \frac{\partial^{2k+1}}{\partial x^{2k+1}} (xT_N')'(1) + (xT_N')(1) \tag{4.11}$$

$$g_N^2(\mu) = \sum_{k=0}^{\infty} \mu^{k} \frac{\partial^{2k}}{\partial x^{2k}} (xT_N')'(1). \tag{4.12}$$

**Lemma 4.2** *Let $f_N^1$, $f_N^2$, $g_N^1$ and $g_N^2$ be defined as in (4.9) - (4.12). Then $f_N^1$ and $f_N^2$, $g_N^1$ and $g_N^2$ form a positive pair.*

*Proof:* One easily checks that

$$\begin{aligned} f_N^1(\mu^2) + \mu \cdot f_N^2(\mu^2) &= f_N(1,\mu) \quad \text{and} \\ g_N^1(\mu^2) + \mu \cdot g_N^2(\mu^2) &= g_N(1,\mu), \end{aligned}$$

where $f_N$ and $g_N$ are Hurwitz polynomials (see Lemma 4.1). This concludes the proof. □

By means of this lemma we immediately obtain the following theorem.

**Theorem 4.1** *The eigenvalues of the spectral operator $A$ are real. One eigenvalue is equal to zero and the remaining $N-1$ eigenvalues are all distinct and have negative sign.*

*Proof:* Let $\mu = \lambda^{-1}$ which induces

$$f_N^1(\lambda^{-1}) = p_1'(1,\lambda) + N^2 \quad \text{and} \quad g_N^1(\lambda^{-1}) = p_2'(1,\lambda) + N^2.$$

We see that $f_N^1$ and $g_N^1$ are identical to the characteristic polynomials. By using Lemma 4.2 we obtain the desired results of our theorem. □

**Remark 4.1** *The result of Theorem (4.1) implicitly contains that our descretization does not introduce spurious modes.*

# 5 Preconditioning

In the following section efficient FD preconditioners for the spectral operator are presented. Here we first consider the one-dimensional case. In order to give a FD preconditioner for $A$ we make use of the representations in (4.3) and (4.4). First we have to find approximations for

$$p''(z_j), \; j = 1, \ldots, N, \quad p'(-1) \text{ und } p'(1).$$

For $p''(z_j)$, $j = 2, \ldots, N-1$, we use the standard central FD scheme, i.e.

$$p''(z_j) \cong 2 \cdot \left( \frac{p(z_{j+1}) - p(z_j)}{z_{j+1} - z_j} - \frac{p(z_j) - p(z_{j-1})}{z_j - z_{j-1}} \right) \cdot \frac{1}{z_{j+1} - z_{j-1}}. \tag{5.1}$$

One observes that (5.1) is equivalent to

$$p''(z_j) \cong a_j p(z_{j-1}) - (a_j + c_j) p(z_j) + c_j p(z_{j+1}), \tag{5.2}$$

where

$$a_j = \frac{\alpha}{s_{j-1} s_{j-\frac{1}{2}}}, \quad c_j = \frac{\alpha}{s_j s_{j-\frac{1}{2}}}$$

and

$$\alpha = \frac{1}{2s_{\frac{1}{2}}s_1}, \qquad s_j = \sin\left(\frac{j\pi}{N}\right).$$

First we try to apply one-sided first order approximations for $p''(z_1)$ and $p''(z_N)$, i.e.

$$p''(z_1) \cong a_2 p(z_1) - (a_2 + c_2)p(z_2) + c_2 p(z_3) \tag{5.3}$$

$$p''(z_N) \cong a_{N-1}p(z_{N-2}) - (a_{N-1} + c_{N-1})p(z_{N-1}) + c_{N-1}p(z_N). \tag{5.4}$$

For $p'(-1)$ and $p'(1)$ we also use one-sided finite differences and obtain:

$$\begin{aligned} p'(1) &\cong \frac{1}{z_1 - z_2} \cdot (p(z_1) - p(z_2)) \\ &= \frac{1}{2s_1 s_{\frac{1}{2}}}(p(z_1) - p(z_2)) \end{aligned} \tag{5.5}$$

and

$$\begin{aligned} p'(-1) &\cong \frac{1}{z_N - z_{N-1}} \cdot (p(z_N) - p(z_{N-1})) \\ &= -\frac{1}{2s_1 s_{\frac{1}{2}}}(p(z_N) - p(z_{N-1})). \end{aligned} \tag{5.6}$$

The FD scheme (5.2)-(5.6) is now associated with an FD operator, here called $A^1_{FD}$.
Now we want to examine the preconditioning properties of $A^1_{FD,0}$. $c = \text{const.} \neq 0$ is obviously an eigenfunction of $A^1_{FD}$ with eigenvalue zero. To check the properties of $A^1_{FD}$ we must eliminate the constant mode. In order to achieve this we introduce a transformation matrix $E$ which is defined by

$$p = Eq,$$

where

$$E = \begin{pmatrix} 1 & 0 & 0 & \cdots & 0 & 0 & 1 \\ 0 & 1 & 0 & \cdots & 0 & 0 & 1 \\ 0 & 0 & 1 & \cdots & 0 & 0 & 1 \\ & \vdots & & \cdots & & \vdots & \\ 0 & 0 & 0 & \cdots & 1 & 0 & 1 \\ 0 & 0 & 0 & \cdots & 0 & 1 & 1 \\ 0 & 0 & 0 & \cdots & 0 & 0 & 1 \end{pmatrix}.$$

We now solve the problem in $q$ and we consider the modified operators

$$\hat{A} = AE, \quad \text{respectively } \hat{A}^1_{FD} = A^1_{FD}E.$$

One can see that $\hat{A}$ and $\hat{A}^1_{FD}$ are identical to $A$ and $A^1_{FD}$ apart from the last column which is now identical to zero. This is because we have chosen the last column to be corresponding to the constant. $E$ can easily be inverted and does not change the structure of the spectral operator. By elimininating the last column and one of the rows (here it is the last one, too) we get a non-singular system in $\mathbb{R}^{N-1,N-1}$. The corresponding spectral or FD operators are called

$$\hat{A}_0 \in \mathbb{R}^{N-1,N-1}, \quad \text{respectively } \hat{A}^1_{FD,0} \in \mathbb{R}^{N-1,N-1}.$$

Table 5.1 contains the eigenvalues of $(\hat{A}^1_{FD,0})^{-1}\hat{A}_0$. We numerically observe that all eigenvalues are real.
One can see that the approximation of first order is a good preconditioner. The minimal eigenvalue is 1 and the maximal eigenvalue approximates $\pi^2/4$, independent of $N$.
Now we want to use finite differences of second order for approximating $p''(z_1)$, $p''(z_N)$, $p'(1)$ and $p'(-1)$. The corresponding FD operator is called $\hat{A}^2_{FD,0}$ and the eigenvalues of $(\hat{A}^2_{FD,0})^{-1}\hat{A}_0$ are presented in table 5.2. Again we numerically obtain real eigenvalues and the minimal eigenvalue is 1. We also see that the maximal eigenvalue approximates $\pi^2/4$. So this approximation yields no advantage compared to our first approximation.

**Table 5.1**

$\lambda_{min}$ and $\lambda_{max}$ of $(\hat{A}^1_{FD,0})^{-1}\hat{A}_0$

| $N$ | $\lambda_{min}$ | $\lambda_{max}$ |
|---|---|---|
| 4 | 1.00 | 1.359246 |
| 8 | 1.00 | 1.966774 |
| 16 | 1.00 | 2.246328 |
| 32 | 1.00 | 2.367677 |
| 64 | 1.00 | 2.421208 |
| 128 | 1.00 | 2.445527 |

**Table 5.2**

$\lambda_{min}$ and $\lambda_{max}$ of $(\hat{A}^2_{FD,0})^{-1}\hat{A}_0$

| $N$ | $\lambda_{min}$ | $\lambda_{max}$ |
|---|---|---|
| 4 | 1.00 | 1.295264 |
| 8 | 1.00 | 1.970879 |
| 16 | 1.00 | 2.249901 |
| 32 | 1.00 | 2.369083 |
| 64 | 1.00 | 2.421703 |
| 128 | 1.00 | 2.445697 |

Figure 5.1 and 5.2 contain a graphical comparison between the method in [4] ( "'N,N-2 method"')

and the just presented method.

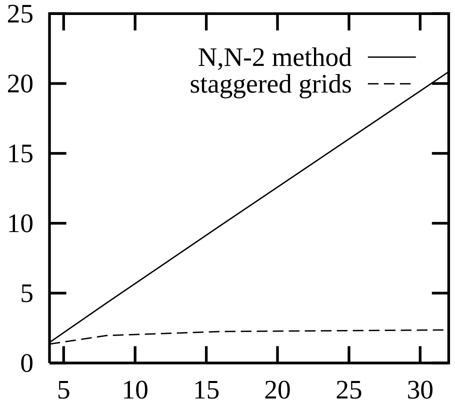


**Figure 5.1:** Maximal eigenvalue of preconditioner $(\hat{A}^1_{FD,0})^{-1}\hat{A}_0$

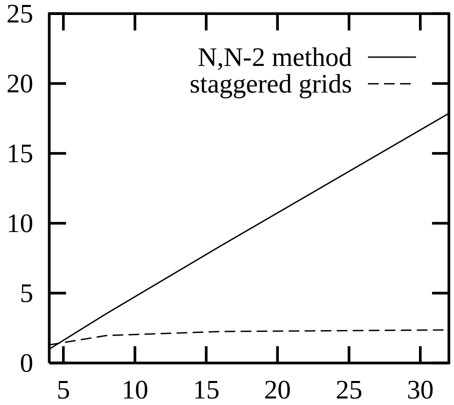


**Figure 5.2:** Maximal eigenvalue of preconditioner $(\hat{A}^2_{FD,0})^{-1}\hat{A}_0$

In relation to these approximations our method has better properties than the N,N-2 method. Finally we employ the spectral scheme for the derivatives $p''(z_1)$, $p''(z_N)$, $p'(1)$ and $p'(-1)$. Due to the corresponding FD operator $\hat{A}^{sp}_{FD,0} \in \mathbb{R}^{N-1,-1}$ we especially use the presentation of (4.4). From table 5.3 it can be seen that the maximal eigenvalue from $(\hat{A}^{sp}_{FD,0})^{-1}\hat{A}_0$ is bounded independent of $N$.

**Table 5.3**

$\lambda_{min}$ and $\lambda_{max}$ of $(\hat{A}^{sp}_{FD,0})^{-1}\hat{A}_0$

| $N$ | $\lambda_{min}$ | $\lambda_{max}$ |
|---|---|---|
| 4 | 1.00 | 1.276142 |
| 8 | 1.00 | 2.228686 |
| 16 | 1.00 | 3.114336 |
| 32 | 1.00 | 3.761935 |
| 64 | 1.00 | 4.167232 |
| 128 | 1.00 | 4.396862 |

Figure 5.3 shows that in the case of the spectral scheme our method with staggered grids has not comparable preconditioner properties as the N,N-2 method. But the maximal eigenvalue is

also bounded independent of $N$.

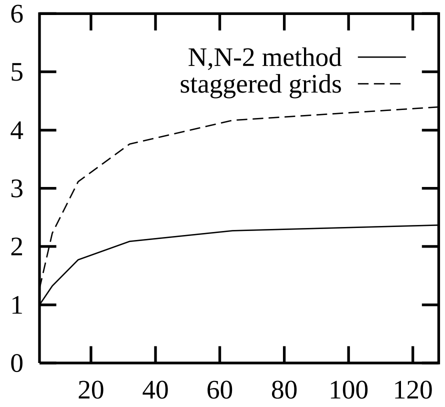


**Figure 5.3:** Maximal eigenvalue of preconditioner $(\hat{A}^{sp}_{FD,0})^{-1}\hat{A}_0$

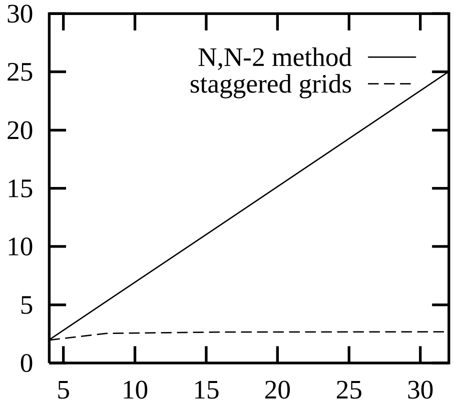


**Figure 5.4:** Maximal eigenvalue of preconditioner $(\hat{A}^{NE}_{FD,0})^{-1}\hat{A}_0$

At last we consider the case that $p'(-1)$ and $p'(1)$ are equal to zero. We obtain the Neumann condition:

$$p'(-1) = p'(1) = 0.$$

By using this boundary condition the FD approximations for $p''(z_1)$ and $p''(z_N)$ now read as follows:

$$\begin{aligned} p''(z_1) &\cong -(a_1 + c_1)p(z_1) + (a_1 + c_1)(z_2) \\ p''(z_N) &\cong -(a_{N-1} + c_{N-1})p(z_{N-1}) + (a_{N-1} + c_{N-1})p(z_{N-2}). \end{aligned}$$

The corresponding FD operator is called $\hat{A}^{NE}_{FD,0}$. Now one can see in figure 5.4 that the maximal eigenvalue of $(\hat{A}^{NE}_{FD,0})^{-1}\hat{A}_0$ is bounded independent of $N$.

**Table 5.4**

$\lambda_{min}$ and $\lambda_{max}$ of $(\hat{A}^{NE}_{FD,0})^{-1}\hat{A}_0$

| $N$ | $\lambda_{min}$ | $\lambda_{max}$ |
|---|---|---|
| 4 | 1.121320 | 1.971857 |
| 8 | 1.019224 | 2.533468 |
| 16 | 1.003583 | 2.663229 |
| 32 | 1.000716 | 2.688467 |
| 64 | 1.000149 | 2.692843 |
| 128 | 1.000032 | 2.693627 |

Similar results can be obtained in the two-dimensional case. Here we only consider the two-dimensional operator for $A^2_{FD,0}$ and $A^{sp}_{FD_0}$ which can be constructed analogously to the spectral operators by means of tensor products.
Let

$$\hat{B} = B(E \otimes E)$$

and

$$
\begin{aligned}
\hat{B}^1_{FD} &= \hat{A}^1_{FD} \otimes E + E \otimes \hat{A}^1_{FD} \\
\hat{B}^{sp}_{FD} &= \hat{A}^{sp}_{FD} \otimes E + E \otimes \hat{A}^{sp}_{FD}.
\end{aligned}
$$

The operators $\hat{B}_0$, $\hat{B}^1_{FD,0}$ and $\hat{B}^{sp}_{FD,0}$ are obtained by eliminating the last column and the last row. One can exstract the eigenvalues of $(\hat{B}^1_{FD,0})^{-1}\hat{B}_0$ and $(\hat{B}^{sp}_{FD,0})^{-1}\hat{B}_0$ from table 5.5 and 5.6.

**Table 5.5**

$\lambda_{min}$ and $\lambda_{max}$ of $(\hat{B}^1_{FD,0})^{-1}\hat{B}_0$

| $N$ | $\lambda_{min}$ | $\lambda_{max}$ |
|---|---|---|
| 4 | 1.00 | 5.425331 |
| 8 | 1.00 | 3.175775 |
| 16 | 1.00 | 2.706077 |

By approximation with FD differences of first order one can see that the maximal eigenvalue of $(\hat{B}^1_{FD,0})^{-1}\hat{B}_0$ approximate the maximal eigenvalue of $(\hat{A}^1_{FD,0})^{-1}\hat{A}_0$.

**Table 5.6**

$\lambda_{min}$ and $\lambda_{max}$ of $(\hat{B}^{sp}_{FD,0})^{-1}\hat{B}_0$

| $N$ | $\lambda_{min}$ | $\lambda_{max}$ |
|---|---|---|
| 4 | 0.929963 | 1.276142 |
| 8 | 0.799335 | 2.228690 |
| 16 | 0.732044 | 3.114336 |

In the case of the spectral scheme we obtain complex eigenvalues and the minimal eigenvalue is less than one. The maximal eigenvalue is close to the maximal eigenvalue of $(\hat{A}^{sp}_{FD,0})^{-1}\hat{A}_0$. Due to the fact that $\hat{A}^{NE}_{FD,0}$ is a tridiagonal matrix one should use this preconditioner in practice. This is the only preconditioner which guarantees that the eigenvalues of the preconditioned operator have still all the same sign.

# 6 The unsteady Stokes equations

## 6.1 The steady case

First we give an example for the solution of (2.1) - (2.3). Let

$$
\bar{x} = \frac{1}{2}(x+1), \quad \bar{y} = \frac{1}{2}(y+1).
$$

Due to the fact that $x$, $y \in [-1,1]$ we know that $\bar{x}$, $\bar{y} \in [0,1]$.

Let us define

$$\begin{aligned} u_1(x,y) &= r(\bar{x})s(\bar{y}), \quad u_2(x,y) = -s(\bar{x})r(\bar{y}) \\ p(x,y) &= \exp(\bar{x}+\bar{y}-1), \end{aligned}$$

where

$$\begin{aligned} r(\bar{x}) &= \bar{x}^2(1-\bar{x})^2 \\ s(\bar{y}) &= 2\bar{y}(1-\bar{y})^2 - 2\bar{y}^2(1-\bar{y}). \end{aligned}$$

Hence the functions $u_1$, $u_2$ satisfy

$$u_1(x,y) = u_2(x,y) = 0 \quad \text{for } (x,y) \in \partial\Omega.$$

Furthermore $r$ and $s$ are choosen such that $r' = s$ and then we derive:

$$\frac{\partial}{\partial x}u_1(x,y) + \frac{\partial}{\partial y}u_2(x,y) = \frac{1}{2}\left(r'(\bar{x})s(\bar{y}) - s(\bar{x})r'(\bar{y})\right) = 0.$$

Therefore the velocity field is divergence free. By substitution of $u_1$, $u_2$ in (2.1) we obtain the right hand side $f$.
Now let $v_1^N$, $v_2^N$ and $q^N$ be the approximations of $u_1$, $u_2$ and $p$. Then we can calculate the absolute errors:

$$ERU1 = ||u_1 - v_1^N||_2, \quad ERU2 = ||u_2 - v_2^N||_2, \quad ERP = ||p - q^N||_2,$$

where

$$||v||_2 = \left[\sum_{i,j=0}^{N} v(x_i,y_j)^2\right]^{\frac{1}{2}} /N, \quad ||q||_2 = \left[\sum_{i,j=1}^{N} p(z_i,w_j)^2\right]^{\frac{1}{2}} /N$$

denotes the discrete $L^2$-Norm in $\Omega$.
We calculate the above errors by taking sufficient time steps until convergence occures; i.e.

$$||u^n - u^{n+1}||_2 \leq 1.0 \cdot 10^{-14}.$$

Table 6.1 presents the results for the Pseudo-Laplacian by using order one methods for the time discretization and the extrapolation of $p$.

| $N$ | $ERU1 = ERU2$ | $ERP$ |
|---|---|---|
| 4 | $4.686 \cdot 10^{-6}$ | $2.355 \cdot 10^{-2}$ |
| 8 | $3.678 \cdot 10^{-12}$ | $3.807 \cdot 10^{-3}$ |
| 12 | $3.555 \cdot 10^{-12}$ | $1.204 \cdot 10^{-3}$ |

**Table 6.1:** Results for the Pseudo-Laplacian

## 6.2 The unsteady case

If $v^{n+1}$ is the exact velocity and $q^{n+1}$ the exact pressure at the time level $t_{n+1}$, we obtain from (2.9) that

$$\frac{\beta_0}{\triangle t}\left(u^{n+1}-v^{n+1}+v^{n+1}-\tilde{u}^{n+1}\right)=\nabla\left(q^{n+1}-p^{n+1}+\bar{p}_l^{n+1}-q^{n+1}\right)\qquad \text{in }\Omega.$$

Since the intermediate velocity $\tilde{u}^{n+1}$ is determined by a $k$-th order time differentiation scheme and the extrapolated pressure by a $l$-th order scheme we observe that the error function

$$u^{n+1}-v^{n+1}+\frac{\triangle t}{\beta_0}\nabla(p^{n+1}-q^{n+1}) \tag{6.1}$$

behaves as

$$O(\triangle t^k)+O(\triangle t^{l+1}).$$

By taking $r=k=l+1$ we finally find out that (6.1) behaves as $O(\triangle t^r)$ for $\triangle t\to 0$.
By combining a backward Euler scheme of second order with a first order extrapolation we totally obtain a second order method in time. This theoretical result is also confirmed by numerical calculations. For that purpose we consider the following example. Let

$$\begin{aligned}u_1(x,y,t)&=z(t)r(\bar{x})s(\bar{y}),\\ u_2(x,y,t)&=-z(t)s(\bar{x})r(\bar{y}),\\ p(x,y,t)&=w(t)\exp(\bar{x}+\bar{y}-1),\end{aligned}$$

where

$$\begin{aligned}r(\bar{x})&=\sin(\pi\bar{x})^2,\\ s(\bar{x})&=r'(\bar{x}),\\ z(t)&=(2\pi-1+\sin(2\pi t))\cdot\frac{1}{2\pi},\\ w(t)&=\cos(2\pi t).\end{aligned}$$

We calculate the mean quadratic errors:

$$\begin{aligned}E_{u_1}&=\max\{ERU1\ :\ t\geq 0\}\\ E_{u_2}&=\max\{ERU2\ :\ t\geq 0\}\\ E_p&=\max\{ERP\ :\ t\geq 0\}.\end{aligned}$$

We only compute these errors when the effect of initialization has disappeared. Then the errors become periodic in time because our functions $z$ and $w'$ are periodic. The numerical results for the case $N=12$ and $\triangle t=\frac{1}{32},\ \frac{1}{64},\ \frac{1}{128}$ and $\frac{1}{256}$ are given in table 6.2 for $r=2$.

| $\triangle t$ | $E_{u_1}$ | $ratio$ | $E_{u_2}$ | $ratio$ | $E_p$ | $ratio$ |
|---|---|---|---|---|---|---|
| $\frac{1}{32}$ | $9.818\cdot 10^{-4}$ | | $1.053\cdot 10^{-3}$ | | $5.831\cdot 10^{-2}$ | |
| $\frac{1}{64}$ | $2.513\cdot 10^{-4}$ | 3.907 | $2.696\cdot 10^{-4}$ | 3.906 | $2.666\cdot 10^{-2}$ | 2.187 |
| $\frac{1}{128}$ | $6.333\cdot 10^{-5}$ | 3.968 | $6.796\cdot 10^{-5}$ | 3.967 | $9.617\cdot 10^{-3}$ | 2.564 |
| $\frac{1}{256}$ | $1.584\cdot 10^{-5}$ | 3.998 | $1.700\cdot 10^{-5}$ | 3.998 | $4.800\cdot 10^{-3}$ | 2.004 |

**Table 6.2:** Results for the Pseudo-Laplacian for $N=12$ and $r=2$

For $r = 3$ this method does not converge because of the use of staggered grids. Therefore we give also the numerical results for the case $k = 1$ and $l = 1$ (see table 6.3).

| $\triangle t$ | $E_{u_1}$ | $ratio$ | $E_{u_2}$ | $ratio$ | $E_p$ | $ratio$ |
|---|---|---|---|---|---|---|
| $\frac{1}{32}$ | $6.477 \cdot 10^{-3}$ | | $6.658 \cdot 10^{-3}$ | | $7.024 \cdot 10^{-2}$ | |
| $\frac{1}{64}$ | $3.268 \cdot 10^{-3}$ | 1.982 | $3.313 \cdot 10^{-3}$ | 2.010 | $3.111 \cdot 10^{-2}$ | 2.258 |
| $\frac{1}{128}$ | $1.647 \cdot 10^{-3}$ | 1.984 | $1.659 \cdot 10^{-3}$ | 1.997 | $1.195 \cdot 10^{-2}$ | 2.603 |
| $\frac{1}{256}$ | $8.281 \cdot 10^{-4}$ | 1.989 | $8.310 \cdot 10^{-4}$ | 1.996 | $4.873 \cdot 10^{-3}$ | 2.454 |

**Table 6.3:** Results for the Pseudo-Laplacian for $N = 12$ and $k = l = 1$

# 7 The Navier-Stokes equations

Now we consider the unsteady Navier-Stokes equations for incompressible flows in velocity-pressure formulation:

$$\begin{aligned}
\frac{\partial u}{\partial t} - \frac{1}{RE}\nabla^2 u + \nabla p + (u \cdot \nabla)u &= f \quad \text{in } \Omega = ]-1,1[^2, && (7.1)\\
\nabla \cdot u &= 0 \quad \text{in } \Omega = ]-1,1[^2, && (7.2)\\
u &= h \quad \text{on } \partial\Omega, && (7.3)\\
u &= u_0 \quad \text{for } t = 0, \quad \text{in } \Omega = ]-1,1[^2. && (7.4)
\end{aligned}$$

As in (2.7)-(2.11) we obtain

$$\begin{aligned}
L^n_{t,2}\tilde{u}^{n+1} - \frac{1}{RE}\nabla^2\tilde{u}^{n+1} + 2\cdot(u^n\cdot\nabla)u^n - (u^{n-1}\cdot\nabla)u^{n-1} + \nabla\bar{p}_1^{n+1} &= f^{n+1} \quad \text{in } \Omega, && (7.5)\\
\tilde{u}^{n+1}_{|\partial\Omega} &= h^{n+1} && (7.6)
\end{aligned}$$

and

$$\begin{aligned}
\frac{3}{2}\cdot\frac{u^{n+1}-\tilde{u}^{n+1}}{\triangle t} + \nabla(p^{n+1} - \bar{p}_1^{n+1}) &= 0 \quad \text{in } \Omega, && (7.7)\\
\nabla \cdot u^{n+1} &= 0 \quad \text{in } \Omega, && (7.8)\\
u^{n+1}\cdot\nu_{|\partial\Omega} &= h^{n+1}\cdot\nu. && (7.9)
\end{aligned}$$

We consider the following example

$$\begin{aligned}
u_1(x,y,t) &= \cos(\gamma t)\cdot\sin\left(\frac{\pi x}{2}\right)\cdot\cos\left(\frac{\pi y}{2}\right),\\
u_2(x,y,t) &= -\cos(\gamma t)\cdot\cos\left(\frac{\pi x}{2}\right)\cdot\sin\left(\frac{\pi y}{2}\right),\\
p(x,y,t) &= \frac{1}{4}\cdot\cos^2(\gamma t)\,(\cos(\pi x)+\cos(\pi y)) + 10(x+y)\cdot\cos(\gamma t).
\end{aligned}$$

Obviously $u_1$ and $u_2$ satisfy $\nabla \cdot u = 0$:

$$\begin{aligned}
\frac{\partial u_1}{\partial x} + \frac{\partial u_2}{\partial y} &= \frac{\pi}{2}\cdot\cos(\gamma t)\cdot\cos\left(\frac{\pi x}{2}\right)\cdot\cos\left(\frac{\pi y}{2}\right) - \frac{\pi}{2}\cdot\cos(\gamma t)\cdot\cos\left(\frac{\pi x}{2}\right)\cdot\cos\left(\frac{\pi y}{2}\right)\\
&= 0.
\end{aligned}$$

The source term $f$ is defined by (7.1), $h$ by (7.3) and the initial condition $u_0$ by (7.4). The Reynolds number is $R = 100$ and to start the time-integration the fields at level $-2\triangle t$, $-\triangle t$ and 0 are equal to the exact solution.

## 7.1 The steady case

First we consider the steady case, i.e. $\gamma = 0$. We compute the following error:

$$E_\phi = ||\phi_N - \phi||_I$$

be the discrete error at the inner collocation points, where

$$||\phi||_I^2 = \frac{1}{(N-1)^2} \cdot \sum_{i,j=1}^{N-1} \phi(x_i, y_j)^2.$$

Table 7.1 contains the results for $\triangle t = 0.01$ and $N = 8$, 12 and 16.

| $N$ | $E_{u_1}$ | $E_{u_2}$ | $E_p$ |
|---|---|---|---|
| 8 | $2.856 \cdot 10^{-7}$ | $2.720 \cdot 10^{-7}$ | $6.350 \cdot 10^{-6}$ |
| 12 | $5.840 \cdot 10^{-12}$ | $4.780 \cdot 10^{-12}$ | $1.075 \cdot 10^{-9}$ |
| 16 | $1.087 \cdot 10^{-14}$ | $1.172 \cdot 10^{-14}$ | $2.105 \cdot 10^{-13}$ |

**Table 7.1:** Results for the Navier-Stokes equations: 2nd order in the steady case

## 7.2 The unsteady case

For the unsteady case we choose $\gamma = 5$, $\triangle t = 0.001$ and $N = 16$. Figure 7.1 demonstrates the temporal evolution of the errors $E_{u_1}$ and $E_p$.

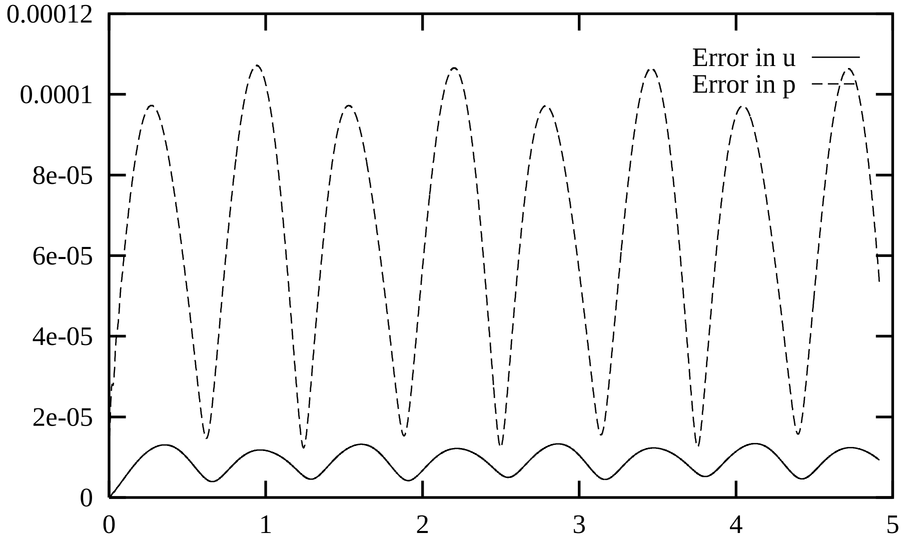


**Figure 7.1:** Temporal evolution of the errors $E_{u_1}$ and $E_p$ for $\triangle t = 0.001$ and $N = 16$.

We observe no amplification of the oscillatiing errors in time, expressing the stability of the numerical solution.

## 7.3 The regularized cavity flow

Finally the regularized cavity flow in the domain $0 \leq \bar{x}, \bar{y} \leq 1$ is computed. On the edge $\bar{y} = 1$ the fluid velocity is

$$\begin{aligned} u_1(\bar{x}, 1) &= -16\bar{x}^2(1-\bar{x})^2 \\ u_2(\bar{x}, 1) &= 0, \end{aligned}$$

where $u_1 = u_2 = 0$ on the other three edges. The source term $f$ is identical to zero.
To compare our results with the results in [2] we have to determine the streamfunction $\psi$ and the vorticity $\omega$. There we have to compute in each time step

$$\omega^{n+1} = \frac{\partial u_2^{n+1}}{\partial \bar{x}} - \frac{\partial u_1^{n+1}}{\partial \bar{y}}.$$

We consider that the steady case is reached when

$$\frac{\max_{i,j} \left|\omega_{i,j}^{n+1} - \omega_{i,j}^{n}\right|}{\triangle t \cdot \max_{i,j} \left|\omega_{i,j}^{n+1}\right|} \leq 2 \cdot 10^{-6}. \tag{7.10}$$

Then we calculate the streamfunction $\psi$ by

$$\nabla^2 \psi = -\omega \quad \text{in } \Omega = ]0,1[^2. \tag{7.11}$$

Table 7.2 displays the maximal time step $\triangle t_c$ for $N = 16$, 20 and 24 for Reynolds numbers $RE = 100$ and 400.

| $N$ | $RE = 100$ | $RE = 400$ |
|---|---|---|
| 16 | 0.303 | 0.104 |
| 20 | 0.250 | 0.074 |
| 24 | 0.234 | 0.056 |

**Table 7.2:** Critical time step $\triangle t_c$ (with an error of $\pm 10^{-3}$).

Table 7.3 contains the maximal value of $|\psi|$ on the inner collocation points $M_1$. $M_1^B$ represents the results in [2].

| $N$ | $RE = 100$ | | $RE = 400$ | |
|---|---|---|---|---|
| | $M_1^B$ | $M_1$ | $M_1^B$ | $M_1$ |
| 16 | $8.3160 \cdot 10^{-2}$ $(0.40 - 0.78)$ | $8.3160 \cdot 10^{-2}$ $(0.40 - 0.78)$ | $8.5777 \cdot 10^{-2}$ $(0.40 - 0.60)$ | $8.5452 \cdot 10^{-2}$ $(0.40 - 0.60)$ |
| 20 | $8.2694 \cdot 10^{-2}$ $(0.42 - 0.73)$ | $8.2695 \cdot 10^{-2}$ $(0.42 - 0.73)$ | $8.5192 \cdot 10^{-2}$ $(0.42 - 0.58)$ | $8.5213 \cdot 10^{-2}$ $(0.42 - 0.58)$ |
| 24 | $8.3315 \cdot 10^{-2}$ $(0.37 - 0.75)$ | $8.3315 \cdot 10^{-2}$ $(0.37 - 0.75)$ | $8.5716 \cdot 10^{-2}$ $(0.43 - 0.63)$ | $8.5715 \cdot 10^{-2}$ $(0.43 - 0.63)$ |
| 32 | $8.3402 \cdot 10^{-2}$ $(0.40 - 0.74)$ | $8.3402 \cdot 10^{-2}$ $(0.40 - 0.74)$ | $8.5480 \cdot 10^{-2}$ $(0.40 - 0.60)$ | $8.4007 \cdot 10^{-2}$ $(0.40 - 0.65)$ |

**Table 7.3:** Maximal value of $|\psi|$. The coordinates of this point are given in brackets.

Table 7.4 shows the corresponding results for $|\omega|$ on the collocation points $M_2$ on the side $\bar{y} = 1$.

| $N$ | $RE = 100$ | | $RE = 400$ | |
|---|---|---|---|---|
| | $M_2^B$ | $M_2$ | $M_2^B$ | $M_2$ |
| 16 | 13.3467 (0.60) | 13.3442 (0.60) | 24.7759 (0.60) | 24.6541 (0.60) |
| 20 | 13.1759 (0.65) | 13.1762 (0.65) | 24.6268 (0.65) | 24.6243 (0.65) |
| 24 | 13.4226 (0.63) | 13.4228 (0.63) | 24.9157 (0.63) | 24.9143 (0.63) |
| 32 | 13.3423 (0.60) | 13.3422 (0.60) | 24.7845 (0.65) | 24.9783 (0.65) |

**Table 7.4:** Maximal value of $|\omega|$. The coordinates of this point are given in brackets.

$M_2$ does not give a precise account of the maximum of $|\omega|$ because of the strong variation of the vorticity on the edge $\bar{y} = 1$ and the uneven spacing of the collocation points. But since the approximation on $\bar{y} = 1$ is done by a polynomial defined at every $\bar{x} \in [0, 1]$ we have divided the space into 201 equally spaced points on this edge. The corresponding values of $|\omega|$ are presented in table 7.5 (denoted $M_3$).

| $N$ | $RE = 100$ | | $RE = 400$ | |
|---|---|---|---|---|
| | $M_3^B$ | $M_3$ | $M_3^B$ | $M_3$ |
| 16 | 13.4476 (0.620) | 13.4434 (0.620) | 25.1604 (0.625) | 25.0222 (0.625) |
| 20 | 13.4441 (0.620) | 13.4441 (0.620) | 24.9273 (0.630) | 24.9241 (0.630) |
| 24 | 13.4446 (0.610) | 13.4565 (0.620) | 24.9148 (0.630) | 24.9010 (0.625) |
| 32 | 13.4448 (0.620) | 13.4430 (0.620) | 24.9109 (0.630) | 25.1123 (0.625) |

**Table 7.5:** Maximal value of $|\omega|$. The coordinates at this point are given in brackets.

# Bibliography


[1] A. Valli A. Quarteroni, *Numerical Approximation of Partial Differential Equations*, Springer-Verlag, Berlin, 1994.

[2] O. Botella, *On the solution of the Navier-Stokes equations using Chebyshev projection schemes with third-order accuracy in time*, Computers & Fluids **26** (1997), 107–116.

[3] A. Lustman D. Gottlieb, *The spectrum of the Chebyshev collocation operator for the heat equation*, SIAM J. Numer. Anal. **20** (1983), 909–921.

[4] W. Heinrichs, *Splitting techniques for the pseudospectral approximation of the unsteady Stokes equations*, SIAM J. Numer. Anal. **30** (1993), 19–39.